

Surface fluxes of bromoform and dibromomethane over the tropical western Pacific inferred from airborne in situ measurements

Liang Feng^{1,2}, Paul I. Palmer^{1,2}, Robyn Butler², Stephen J. Andrews³, Elliot L. Atlas⁴, Lucy J. Carpenter³, Valeria Donets⁴, Neil R. P. Harris⁵, Ross J. Salawitch⁶, Laura L. Pan⁷, Sue M. Schauffler⁷

1) National Centre for Earth Observation, University of Edinburgh, Edinburgh, UK

2) School of GeoSciences, University of Edinburgh, Edinburgh, UK

3) Department of Chemistry, Wolfson Atmospheric Chemistry Laboratories, University of York, UK

4) University of Miami, Florida, USA

5) Centre for Atmospheric Informatics and Emissions Technology, Cranfield University, Cranfield, UK

6) University of Maryland, College Park, Maryland, USA

7) National Center for Atmospheric Research, Boulder, Colorado, USA

Corresponding author: Paul I. Palmer (paul.palmer@ed.ac.uk)

ABSTRACT

We infer surface fluxes of bromoform (CHBr_3) and dibromoform (CH_2Br_2) from aircraft observations over the western Pacific using a tagged version of the GEOS-Chem global 3-D atmospheric chemistry model and a Maximum A Posteriori inverse model. Using GEOS-Chem as an intermediary, we find that the distribution of *a priori* ocean emissions of these gases are reasonably consistent with observed atmospheric mole fractions of CHBr_3 ($r=0.62$) and CH_2Br_2 ($r=0.38$). These *a priori* emissions result in a positive model bias in CHBr_3 peaking in the marine boundary layer, but capture observed values of CH_2Br_2 with no significant bias by virtue of its longer atmospheric lifetime. Using GEOS-Chem, we find that observed variations in atmospheric CHBr_3 are determined equally by sources over the western Pacific and those outside the study region, but observed variations in CH_2Br_2 are determined mainly by sources outside the western Pacific. Numerical closed-loop experiments show that the spatial and temporal distribution of boundary layer aircraft data have the potential to substantially improve current knowledge of these fluxes, with improvements related to data density. Using the aircraft data, we estimate aggregated regional fluxes of $3.6 \pm 0.3 \times 10^8$ g/month and $0.7 \pm 0.1 \times 10^8$ g/month for CHBr_3 and CH_2Br_2 over 130° — 155°E and 0° — 12°N , respectively, which represent reductions of 20—40% and substantial spatial deviations from different *a priori* inventories. We find no evidence to support a robust linear relationship between CHBr_3 and CH_2Br_2 oceanic emissions, as used by previous studies.

40 1.Introduction

The role of halogens in the catalytic destruction of stratospheric ozone is well established (WMO, 2014). The anthropogenic contribution to the inorganic halogen budget continues to decline in the stratosphere as a result of the Montreal protocol. A consequence of this decline
45 is that very short-lived substances (VSLS), halogenated compounds with e-folding lifetimes typically much less than 6 months, now represent a proportionally greater source of stratospheric halogens. The wide range of VSLS atmospheric lifetimes allows at least some of the emitted material to reach the upper troposphere, particularly over geographical regions where there is rapid, deep convection (Penkett et al., 1998; Yang et al., 2005; Warwick et al.,
50 2006; Levine et al., 2007; Pisso et al., 2010; Hosking et al., 2010; Carpenter et al., 2014; Hossaini et al., 2016a; Butler et al., 2016). Here, we use aircraft observations of bromoform (CHBr_3) and dibromomethane (CH_2Br_2) collected over the western Pacific Ocean to infer, using an inverse model, the magnitude and distribution of ocean emissions of these gases.

55 There is a wide range of VSLS that are beginning to limit the recovery of stratospheric ozone (e.g., Read et al., 2008; Hossaini et al., 2015; Oman et al., 2016). Chlorine VSLS are typically dominated by anthropogenic sources, but the fraction depends on the species (Hossaini et al., 2016b). Their natural sources include biomass burning, phytoplankton production, and soils. Iodine and bromine VSLS have predominately natural sources. Iodine VSLS are mainly from
60 ocean production processes, but with lifetimes of only a few days they are too reactive to be transported out of the marine boundary layer in large quantities. Bromine VSLS are also mainly from natural ocean sources (Gschwend et al., 1985; Manley et al., 1992; Sturges et al., 1992; Tokarczyk et al., 1994; Warwick et al., 2006; Carpenter and Liss, 2000; 2009; Palmer et al., 2009; Quack and Suess, 1999; Quack and Wallace, 2003; Quack et al., 2007; Butler et al.,
65 2007; Leedham et al., 2013). The most abundant bromine VSLS species are CHBr_3 and CH_2Br_2 . Together they account for about 80% of bromine VSLS in the marine boundary layer (Law and Sturges, 2007; O'Brien et al., 2009; Hossaini et al., 2013). The local atmospheric lifetime for CHBr_3 , determined by OH oxidation (76 days) and photolysis (36 days), is 24 days. CH_2Br_2 has a longer atmospheric lifetime of about 123 days, determined primarily by OH
70 oxidation (123 days) and to a much lesser extent by photolysis (5000 days). Their lifetimes are sufficiently long that these natural halogenated compounds can be transported to the upper troposphere.

75 Previous measurement campaigns have reported that bromine VLSL and their degradation products represent 2-8 pptv of stratospheric inorganic bromine (e.g., Dorf et al., 2008; Salawich et al., 2010). Complementary model simulations of atmospheric chemistry and transport, driven by *a priori* ocean emission inventories, report similar values (2-7 pptv) that are determined mainly by localized regions of active ocean biology that coincide with strong convection. Example regions include western Pacific Ocean, tropical Indian Ocean, and off
80 the Pacific coast of Mexico. These model calculations also suggest that 15-75% of the stratospheric bromine budget from bromine VLSL is delivered by the direct transport of the emitted halogenated compounds (Liang et al., 2010; Hossaini et al., 2016a; Aschmann et al., 2009). The large range of values reflects uncertainty in ocean emissions, model transport, and the wet deposition of degradation products in the upper troposphere lower stratosphere.

85 Current knowledge of ocean emissions of CHBr_3 and CH_2Br_2 are poorly constrained by the sparse measurements. Bottom-up and top-down methods have been used to estimate global CHBr_3 and CH_2Br_2 emissions. The bottom-up approach assumes local flux estimates are representation of larger spatial scales. Ship-borne air-sea flux observations with limited spatial
90 and temporal coverage are extrapolated over ocean basins (e.g. Quack and Wallace, 2003; Carpenter and Liss, 2000; Butler et al., 2007; Ziska et al., 2013). Poor observation coverage results in fluxes that rely heavily on assumptions used for extrapolation (Stemmler et al, 2015).

The top-down method, in this application, uses an atmospheric chemistry transport model to
95 describe the relationship between emissions and the atmospheric measurements. The model emissions are fitted to the observations by adjusting their magnitude until the discrepancy between the model and observed atmospheric measurements is minimized. This fitting can be achieved using heuristic techniques or more established Bayesian optimization methods (e.g. Liang et al, 2010, Ordonez et al, 2012, Ashfold et al., 2015). The short atmospheric
100 lifetime of CHBr_3 poses particular difficulties for the top-down approach because atmospheric mole fractions are highly variable (Ashfold et al., 2015). Some studies have introduced (explicitly or implicitly) a simple linear correlation between CHBr_3 and CH_2Br_2 emissions to provide an additional constraint on the CHBr_3 flux estimate (e.g. Liang et al., 2010, Ordóñez et al., 2012). This approach, however, is then subject to errors associated with the assumption
105 about the correlation. As with the bottom-up method, the top-down method is subject to errors due to poor spatial and temporal coverage of observations. By virtue of various assumptions made (and justified) by individual studies the resulting bottom-up and top-down CHBr_3 and CH_2Br_2 fluxes are significantly different (e.g. Hossaini et al., 2016a). For example, the estimated global CHBr_3 annual emissions range from 216 Tg (Ziska et al., 2013) to 530 Tg
110 (Ordóñez et al., 2012).

We use data from two coordinated aircraft campaigns over the western Pacific during 2014 to infer regional emission estimates of CHBr_3 and CH_2Br_2 for the campaign period using a Bayesian inverse model. The Co-ordinated Airborne Studies in the Tropics (CAST; Harris et al., 2017), and CONvective Transport of Active Species in the Tropics (CONTRAST; Pan et al., 2016) campaigns measured a suite of trace gases and aerosols centred on the Micronesian region in the western Pacific, including Guam, Chuuk, and Palau during January and February 2014. We interpret aircraft measurements of CHBr_3 and CH_2Br_2 mole fraction using the GEOS-Chem atmospheric chemistry transport model and a Maximum A Posteriori (MAP) inverse model approach.

In the next section we describe the CAST and CONTRAST CHBr_3 and CH_2Br_2 mole fraction data, the GEOS-Chem atmospheric chemistry transport model used to interpret the data, and the MAP inverse model. In section 3, we report a model comparison with the CAST and CONTRAST atmospheric data, and results from the MAP inversion. We conclude the paper in section 4.

2. Data and Methods

We use CHBr_3 and CH_2Br_2 mole fraction determined using GC/MS from whole air sample (WAS) canisters collected during the CAST and CONTRAST aircraft campaigns during January 18th to February 28th, 2014 (Harris et al., 2017; Pan et al., 2016). We refer the reader to Andrews et al. (2016) for a more detailed description of the observation data sets, and to Butler et al (2016) for a statistical analysis of the CHBr_3 and CH_2Br_2 mole fraction data. For CAST, WAS canisters were filled aboard the Facility for Airborne Atmospheric Measurements (FAAM) BAe-146 UK Atmospheric Research Aircraft. These canisters were analysed for CHBr_3 and CH_2Br_2 and other trace compounds within 72 hours of collection. The WAS instrument was calibrated using the National Oceanic and Atmospheric Administration (NOAA) 2003 scale for CHBr_3 and the NOAA 2004 scale for CH_2Br_2 (Jones et al., 2011; Andrews et al., 2016). For CONTRAST, a similar WAS system was employed to collect CHBr_3 and CH_2Br_2 measurements on the NSF/NCAR Gulfstream-V HIAPER (High-performance Instrumented Airborne Platform for Environmental Research) aircraft. A working standard was used to regularly calibrate the samples, and the working standard was calibrated using a series of dilutions of high concentration standards that are linked to National Institute of Standards and Technology standards. The mean absolute percentage error for CHBr_3 and CH_2Br_2 measurements (over the altitude range 0–8 km) is 7.7% and 2.2%, respectively,

between the two WAS systems and two accompanying GC/MS instruments used by CAST and CONTRAST.

150 To interpret these atmospheric data we use the GEOS-Chem global 3-D atmospheric
chemistry transport model (v9.03, <http://geos-chem.org>). We drive the GEOS-Chem model
using GEOS-FP meteorological fields, provided by the Global Modeling and Assimilation
Office at NASA Goddard, with a horizontal resolution of 2° (latitude) X 2.5° (longitude). We use
a tagged version of the model (Butler et al, 2016) in which the atmospheric chemistry is
155 linearized by using pre-computed OH and photolysis loss terms using the same version of the
model but with a more complete description of HOx-NOx-Ox and bromine chemistry (Parrelle
et al., 2012). Our 3-D OH fields are consistent with the observed methyl chloroform lifetime.
We find small (5%) adjustments to these OH fields do not significantly affect our analysis or
conclusions (not shown). For the purpose of our calculations we pre-compute these loss terms
160 every three hours during the campaign. This tagged modelling approach greatly simplifies the
calculation of the Jacobian matrix used by the inverse model to determine surface flux
estimates, as described below. We have previously evaluated this version of the model using
CHBr₃ and CH₂Br₂ mole fraction data from NOAA/ESRL (Butler et al, 2016), and showed a
level of agreement with *in situ* observations that is comparable to the ensemble of models
165 reported by Hossaini et al (2016a).

We use *a priori* emissions of CHBr₃ and CH₂Br₂ from the Ordóñez et al (2012) inventory, which
is based on the top-down methodology using aircraft observations from 1996 to 2006. This
represents one of three commonly used inventories, which were recently evaluated in a multi-
170 model inter-comparison study (Hossaini et al, 2016a). Liang et al (2010) also employed a top-
down methodology to infer CHBr₃ and CH₂Br₂ fluxes, but Ziska et al. (2013) inferred these
fluxes from a database of surface ocean observations collected from 1989 to 2011. We find
no single inventory is best at reproducing observations of both gases. Ordóñez et al (2012)
assumed a linear relationship between tropical CHBr₃ and CH₂Br₂ emissions and monthly
175 fields of chlorophyll-a, a proxy for ocean biological activity, to help fill in the spatial and
temporal gaps left by the aircraft data. This approach strongly links the distributions of these
two gases in the *a priori* inventory, an assumption we examine below. We primarily use
Ordóñez et al. (2012) but also show the results from other inventories. For our study period,
these aggregated regional fluxes are 6.2x10⁸ g/month and 0.9±0.2x10⁸ g/month for CHBr₃ and
180 CH₂Br₂ over 130°—155°E and 0°—12°N, respectively.

Figure 1 shows the geographical regions considered in this study. We divide the world into
605 basis functions: 1) a nested domain of 600 grid-scale tagged regions over the tropical

western Pacific (105°—165°E, 15°S—25°N); 2) a lateral boundary of 15° surrounding the
 185 nested domain, described by four tagged regions; and 3) the rest of the world. We spin-up the
 model using *a priori* inventories (Ordóñez et al., 2012) from July 1st 2013 to January 18th 2014,
 reducing the impact of initial conditions.

We use the MAP approach to infer CHBr₃ and CH₂Br₂ surface fluxes from atmospheric mole
 190 fraction measurements taken by CAST and CONTRAST aircraft campaigns. We infer regional
 monthly mean surface fluxes, f , of CHBr₃ and CH₂Br₂:

$$f_p^g(x) = f_0^g(x) + \sum_i c_i^g BF_i^g(x), \quad (1)$$

where superscript g denotes trace gas, and the subscripts 0 and p denote the *a priori* and *a*
posteriori state vector, respectively. We describe the regional fluxes as a product of a basis
 195 function set $BF_i^g(x)$, representing distributions of monthly mean fluxes of the study gases over
 605 pre-defined geographic regions (Figure 1) over the duration of the CAST and CONTRAST
 aircraft experiments, and scalar coefficients c_i^g that are fitted to the data.

We include all the coefficients c_i^g for the pre-defined 605 basis functions into the state vector
 200 \mathbf{c} that describes the CHBr₃ and CH₂Br₂ fluxes, which we fit to the observations. We take into
 account the uncertainty of the model spin-up by including a scaling factor into the state vector
 to adjust the background (initial) field, assuming that the model describes the background
 vertical structure over the study domain. As a result the state vector \mathbf{c} has a total of 606
 elements. We optimally estimate the state vector \mathbf{c} by minimizing the associated cost function
 205 $J(\mathbf{c})$:

$$J(\mathbf{c}) = \frac{1}{2}[\mathbf{c} - \mathbf{c}_0]^T \mathbf{B}^{-1}[\mathbf{c} - \mathbf{c}_0] + \frac{1}{2}(\mathbf{y}_{obs} - H(\mathbf{c}))^T \mathbf{R}^{-1}(\mathbf{y}_{obs} - H(\mathbf{c})), \quad (2)$$

where the superscripts T and -1 denote the matrix transpose and inverse operations,
 respectively; \mathbf{c}_0 represents the *a priori* estimates; and \mathbf{B} represents the *a priori* error covariance
 matrix. The measurement vector, including the CAST/CONTRAST CHBr₃ and CH₂Br₂ mole
 210 fraction data, is denoted by \mathbf{y}_{obs} , and \mathbf{R} is the measurement error covariance matrix. The
 forward model H projects the state vector (scalar coefficients) into observation space (3-D
 mole fractions), and includes the GEOS-Chem atmospheric chemistry and transport model
 that is sampled at the time and location of each observation.

215 We assume a 60% uncertainty for fluxes within the nested domain and a 50% uncertainty for
 fluxes in the lateral boundary and the rest of the world regions, guided by the discrepancy
 between the top-down and bottom-up inventories and their limited spatial and temporal
 variation. We also assume that the *a priori* errors within the nested domain are correlated over
 a distance of 400 km, corresponding to approximately the width of two adjacent grid boxes.

220 We assume the initial conditions for the mole fractions have a 30% uncertainty. We assume individual observations of CHBr_3 and CH_2Br_2 have errors of 20% and 10%, respectively, and are uncorrelated. These conservative values are guided by an analysis of data collected from different instruments during CAST and CONTRAST (Andrews et al, 2016). We assume that the observation error covariance \mathbf{R} is diagonal, which also includes model error, such as the
 225 representation error and the errors in modelling atmospheric transport and chemistry processes, with an assumed value of 20%. Our results over the geographical regions with dense observation coverage are insensitive to different assumptions about *a priori* uncertainty and observation errors. For example, our changing the *a priori* emission uncertainty by $\pm 20\%$, results in changes in the aggregated *a posteriori* CHBr_3 emission (130° — 155°E and 0° — 12°N)
 230 of typically less than 10%.

The Jacobian matrix describes the sensitivity of atmospheric CHBr_3 and CH_2Br_2 CAST and CONTRAST measurements to changes in geographical surface emissions and the initial value on January 18th 2014. We construct it by scaling the tagged tracers originating from a specific
 235 geographical region by surface fluxes from that region.

To avoid negative flux estimates due to, for example, an uneven distribution of observations we use value-dependent *a priori* uncertainties for grid point flux estimates. We assume a functional form for the uncertainty of the flux coefficient c_i (equation 1):

$$240 \quad \sigma(c_i) = \begin{cases} 0.8, & c_i > -0.6 \\ 0.8 - 2(-0.6 - c_i)e^{k(1.0+c_i)}, & c_i < -0.6, \end{cases} \quad (3)$$

where k ($=3$) is a pre-chosen factor that defines the gradient of the uncertainty with respect to the change of c_i . Using this approach, the *a priori* uncertainty decreases rapidly towards zero when c_i becomes smaller than -0.6 (i.e., when the flux estimate is smaller than 40% of the *a priori*). We find that using different parameters (e.g. changing the threshold from -0.6 to -0.8)
 245 does not significantly change our flux estimates.

3 Results

Forward Model Analysis

250 Figure 2 shows that the model overestimates the CHBr_3 concentrations by 0.1—0.7 pptv at altitudes from 0.5 to 12.5 km, with the largest values near the surface that reflects errors in a *a priori* ocean fluxes (Hossaini et al., 2016a; Butler et al, 2016). The model has reasonable skill at reproducing the mean observed vertical gradient ($r=0.62$) but has a positive model bias of 0.46 ± 0.39 pptv. We find that vertical variations in CHBr_3 are determined approximately equally

255 by sources over the western Pacific study region (Figure 1) and by sources immediately
outside of the nested domain and further afield (Butler et al, 2016). These contributions show
different vertical structures. The contribution from fresher sources over the western Pacific has
a steeper atmospheric lapse rate from the boundary layer to the free troposphere than the air
masses from neighbouring regions. Both contributions are approximately uniform above the
260 free troposphere, with the exception of a peak at 10-12 km from the air being transported into
the nested domain (Butler et al, 2016). These differences in vertical structure help the
inversion system identify the origin of CHBr₃ at different vertical levels.

The model reproduces some of the observed CH₂Br₂ variation ($r=0.38$) but with a small mean
265 bias (0.01 ± 0.14 pptv). Figure 2 shows that the CH₂Br₂ source outside the nested domain
represent more than 60% (0.7—0.9 pptv) of the values sampled over the western Pacific, and
almost invariant with altitude. This is due to weaker surface emissions over the western Pacific
and the longer atmospheric lifetime of CH₂Br₂ compared to CHBr₃. Ocean emissions from the
western Pacific and from the immediate neighbouring regions each contribute only 0.1—0.3
270 pptv to CH₂Br₂. This highlights the difficulties of inferring ocean fluxes of CH₂Br₂ only using
atmospheric CH₂Br₂ data collected over the western Pacific and considering this region in
isolation.

To examine model transport errors associated with using a relatively coarse model spatial
275 resolution ($2^\circ\times 2.5^\circ$), we ran a short, high-resolution ($0.25^\circ\times 0.3125^\circ$) simulation of CHBr₃ over
a limited spatial domain centred on the western Pacific and compared that against the
CAST/CONTRAST data. We acknowledge that we could still miss rapid, sub-grid scale
convective events using this model that has a factor-of-eight improvement in spatial resolution.
However, we find that differences between the two model runs are much smaller than the
280 differences between the individual model runs and the observations (Figure 2). Figure 2 also
shows that the global and nested GEOS-Chem simulations of CHBr₃ and CH₂Br₂ mole
fractions, corresponding to our the *a posteriori* flux estimates (Figure 4), are more consistent
with the observations than *a priori* fluxes. This result demonstrates that the *a priori* model bias
can be explained by, in principle, errors in ocean sources.

285

Closed-Loop Numerical Experiments

In the absence of independent observations to evaluate our *a posteriori* ocean fluxes we use
closed-loop numerical experiments to understand what we can theoretically achieve from
CAST and CONTRAST data, accounting for a realistic description of model and measurement
290 errors. These calculations, often called observing system simulation experiment (OSSEs),
provide an upper boundary on the ability of available data to infer the true state.

First, we generate synthetic observations at the time and location of the CAST and CONTRAST data by sampling 3-D model fields of CHBr_3 and CH_2Br_2 mole fraction driven by the *a priori* inventories, which we regard as the ‘true’ emissions. We consider these sample mole fraction values as the instrument observation after we superimpose instrument (unbiased) noise, informed by realistic observation uncertainty. Second, we enlarge the (‘true’) *a priori* emissions to generate the *a priori* estimate for the OSSEs: by 50% for emissions over the western Pacific and by 30% for emissions from the neighbouring region. The resulting atmospheric mole fractions represent our model *a priori* concentrations. With perfect coverage of the atmosphere with perfect data (i.e. infinitesimal noise levels) fitting model emissions to the true observations would result in estimating the true ocean emissions. We describe our results as the difference between the *a posteriori* and true fluxes using a metric (Palmer et al, 2000; Feng et al, 2009) that describes the error reduction $\gamma = 1 - \sigma_a/\sigma_f$, where σ_a and σ_f denote the *a posteriori* and *a priori* uncertainties, respectively, ignoring the correlation between state vector elements. The closer the value of γ is to unity the larger reduction in uncertainty.

Figure 3 shows that the CAST/CONTRAST CH_2Br_2 and CHBr_3 measurements can reproduce the true fluxes, mainly between 130-155°E and 3S°-15°N, by reducing the inflated *a priori* flux estimate. *A posteriori* fluxes in several grid boxes are lower than the true value, which is a result of regions overcompensating for other regions that have insufficient data to estimate their emissions. Regions influenced with fewer measurements (Figure 1) generally have smaller reductions in error, as expected. The error reductions for CHBr_3 range from 0.1 to 0.6 over the study domain, reflecting the widespread sensitivity of the CAST and CONTRAST observations to emissions from the tropical western Pacific region. The mean and median *a posteriori* fluxes are approximately a factor of three closer than the *a priori* to the true fluxes, with a 40% improvement in the uncertainties. In contrast, for CH_2Br_2 , the error reduction is much smaller, with values greater than 0.3 only over a small geographical region where the data density is greatest. There is a factor-of-two improvement in the discrepancy of the fluxes with the ‘true’, and a 30% improvement in the uncertainties. This large improvement in the knowledge of flux estimates is partly due to our simple description of the difference between the true and *a priori* field.

Ocean Emissions of CHBr_3 and CH_2Br_2 Inferred from CAST/CONTRAST data

We now examine the fluxes inferred from the CAST and CONTRAST measurements. Figure 4 shows elevated *a posteriori* CHBr_3 emissions surrounding small islands north of the tropics, such as Palau (7.4°N, 134.5°E) and Chuuk (7° 25' N, 151° 47' E). However, we find that

emissions surrounding Guam (13.5°N, 144.8°E) are not significantly different from the adjacent open ocean. This reflects the distribution of boundary layer measurements (altitudes <2.5 km) of CHBr₃ observed during CAST and CONTRAST flights (Figure 1). We find that through sensitivity experiments (described below) that the *a posteriori* emissions are inferred by data and not via spatial correlations in the *a priori* emission inventory. Our *a posteriori* CHBr₃ emissions are generally higher than the bottom-up estimates from Ziska et al (2013), particularly over north of tropics.

We find that our *a posteriori* CH₂Br₂ emission estimates are lower than *a priori* estimates over open oceans north of 5°N. We also find elevated fluxes around islands and part of open oceans south of 5°N. Similar to CHBr₃, these elevated fluxes coincide with large boundary layer measurements from CAST and CONTRAST.

Over the study domain (130°—155°E and 0°—12°N) our *a posteriori* fluxes are $3.6 \pm 0.3 \times 10^8$ g/month and $0.7 \pm 0.1 \times 10^8$ g/month for CHBr₃ and CH₂Br₂, respectively. These represent reductions of 40% and 20% relative to the *a priori* values, respectively. We find that our flux estimates are largely insensitive to small changes in the assumed observation and *a priori* errors. The corresponding *a posteriori* mole fractions of CHBr₃ and CH₂Br₂ (not shown) have smaller mean biases (-0.03 ± 0.22 pptv, -0.1 ± 0.11 pptv) and improved correlations ($r=0.74$, $r=0.56$) than the *a priori* values compared to the observations. The small negative bias of -0.03 pptv in our *a posteriori* model simulation mainly reflects values in to the upper troposphere (Figure 2), where measurements are less sensitive to local surface fluxes.

This model bias may reflect unaccounted atmospheric model transport error, particularly because we use a relatively coarse atmospheric transport compared to the data resolution. Previous studies have highlighted similar issues (e.g. Russo et al, 2015). Figure 3 shows, however, that CAST and CONTRAST data can only reduce flux uncertainties by about 10—60% over the study regions at this coarse model resolution, limited by the density and coverage of the available data. Using a consistent model simulation but run at a higher spatial resolution ($0.25^\circ \times 0.3125^\circ$) we find significant improvement in model performance (Figure 2). This provides some evidence that our *a posteriori* emission estimates are robust against the resolution of the meteorological input data. We also find that using this high-resolution model does not significantly reduce the small bias above 8 km. This may point to a small offset between CAST (mostly at lower altitudes <8 km) and CONTRAST measurements (more at higher altitudes) (Andrews et al., 2016). Systematic errors between CAST and CONTRAST data are difficult to fully quantify, but any possible small offset between CAST and CONTRAST data is unlikely to affect our results significantly. Our sensitivity experiments (not shown), in

365 which we introduce a bias between CONTRAST and CAST data that we infer in our inversion,
show similar results to our control experiment configuration.

The spatial gradient we find in our *a posteriori* CHBr_3 emissions between the coasts of Palaua
and Chuuk and the surrounding open oceans is not present in our *a priori* emission inventory
370 (Ordóñez et al, 2012). It is, however, qualitatively consistent with observations (e.g., O'Brien
et al., 2009; Quack et al., 2007) and bottom-up estimates (e.g., Ziska et al., 2013 and
Simmerler et al., 2015). These elevated coastal emissions also improve the fit to CAST and
CONTRAST observation particularly between 6-10 km. Figure 4 shows that the spatial
distribution of *a priori* and *a posteriori* CH_2Br_2 emissions from the open ocean is different from
375 the climatological bottom-up emissions (Ziska et al, 2013), particularly south of 5°N . This is
surprising because studies have shown that tropical ocean emissions of CH_2Br_2 are correlated
with the distribution of chlorophyll-a (e.g., Liu et al., 2013), but differences may reflect inter-
annual changes in ocean biology.

380 Figure 5 shows the *a priori* and *a posteriori* $\text{CHBr}_3:\text{CH}_2\text{Br}_2$ flux ratios. The top down inventory
of Ordóñez et al (2012) use a linear model to describe emissions from these two gases, but
the bottom-up inventory by Ziska et al, (2013) develop the emissions independently using a
database of ocean observations. This discrepancy between the two inventories is why we
chose not to exploit this linear relationship in our MAP inversion. Our *a posteriori* emissions
385 for CHBr_3 and CH_2Br_2 appear to be linearly related at low emissions but larger values appear
to follow a more complicated relationship, which may reflect differences in the responsible
ocean biological processes.

To examine the sensitivity of our results to the *a priori* inventories, we use the same MAP
390 approach to infer CHBr_3 flux from CAST and CONTRAST measurements for three different
prior inventories (Figure 6): (a) Ziska et al (2013); (b) Liang et al (2010); and (c) Ordóñez et al
(2012). For simplicity, we assume the same *a priori* error covariance for the 600 grid boxes
over the tropical western Pacific (Figure 1) when the three different priori inventories are used.
Figure 6 shows that despite a large *a priori* discrepancy, the three sets of *a posteriori* flux
395 estimates (Figure 6) show similar features over our study domain between $130^\circ\text{--}155^\circ\text{E}$ and
 $0^\circ\text{--}12^\circ\text{N}$ (as denoted by white rectangles). Despite their being a large discrepancy between
 CHBr_3 ocean emission estimates over our study region from Ziska et al., (2013) (0.73×10^8
g/month) and Liang et al., (2010) (6.9×10^8 g/month) inventories, we infer similar aggregated
a posteriori emissions of 3.0×10^8 g/month and 3.5×10^8 g/month from Ziska et al., (2013) and
400 Liang et al., (2010), respectively. This suggests that the choice of *a priori* plays only a small
role in determining the *a posteriori* solution. These *a posteriori* estimates are also comparable

with fluxes from our control experiment ($3.6 \pm 0.3 \times 10^8$ g/month) that uses *a priori* emissions from Ordóñez et al., (2012). We find that outside our study domain, the model-observation discrepancies are still very large, in particular over coastal regions, due to the limited
405 observation coverage by CAST and CONTRAST experiments.

410 **4. Summary and Concluding Remarks**

Very short-lived brominated gases have predominately natural sources, and therefore cannot be regulated by international agreements (Oman et al., 2016; Butler et al., 2007). Current understanding of these natural sources is poor due to the infrequent and incomplete
415 measurements of ocean fluxes that vary in space and time. Past studies have relied on developing bottom up inventories using a database of ship-borne measurements or an heuristic top down method that adjusted *a priori* emissions to match tropospheric and lower stratospheric measurements of a range of gases, including of CHBr_3 and CH_2Br_2 . As a consequence of the uncertainties associated with the modelling and data, the resulting
420 inventories adopt simple distributions and are not necessarily consistent with each other on regional spatial scales.

Here, we used an *a priori* inventory to reproduce observed atmospheric boundary layer variations of CHBr_3 and CH_2Br_2 over a small geographical region encompassing Guam, Palau
425 and Chuuk over the western Pacific. The measurements were collected as part of the CAST and CONTRAST aircraft campaigns during January and February 2014. We use the GEOS-Chem atmospheric chemistry model to relate the *a priori* emissions to the atmospheric concentrations, and develop a MAP inverse model to infer the ocean fluxes that correspond with the aircraft measurements.

430

First, using a small number of closed-loop numerical experiments we showed that the aircraft data could in theory, using assumptions about their uncertainties, improve knowledge of ocean fluxes. Improvements in knowledge are generally related to the density of measurements, as expected.

435

Using the aircraft data we find substantial spatial variations in fluxes of both gases that differ significantly from the *a priori* inventory. We find that aggregated regional *a posteriori* fluxes of CHBr_3 ($3.6 \pm 0.3 \times 10^8$ g/month) and CH_2Br_2 ($0.7 \pm 0.1 \times 10^8$ g/month) are 40% and 20% lower than

the *a priori* fluxes over the main study domain (130°—155°E and 0°—12°N). Using the model we find that observed variations of CHBr_3 are determined mainly by the open ocean while CH_2Br_2 has a large influence from outside the immediate study region. *A posteriori* fluxes significantly improve the mean observed vertical gradient of both gases, particularly in the free troposphere. We also find no evidence to suggest a robust linear relationship between the emissions of these two gases over the study region, unlike one of the top-down *a priori* inventories. This discrepancy may reflect differences in the analysis of data over different spatial scales, or the construction of the *a priori* inventory using data in the free and upper troposphere where observed air masses originating from disparate surface sources have time to mix.

The MAP approach we used fits *a posteriori* fluxes to minimize the discrepancy between model and observed atmospheric mole fractions. Any discrepancy in atmospheric data may result from errors in surface fluxes (emissions minus uptake), atmospheric chemistry, and atmospheric transport. Where observation coverage is denser, our inversion results are less sensitive to the assumed *a priori* inventories, as expected. The next most likely source of error is atmospheric transport, particularly sub-grid scale vertical mixing. Sensitivity tests that crudely account for model errors suggest that the *a posteriori* fluxes are robust.

Our paper highlights the value of using atmospheric data to improve the magnitude and distribution of ocean emissions of halogenated gases, but also shows some of the difficulties associated with interpreting these data even with the aid of an atmospheric transport model. Future scientific progress in quantitatively understanding the role of natural emissions of halogens in the catalytic destruction of stratospheric ozone is hampered by the lack of available observations.

465 **Author contributions.**

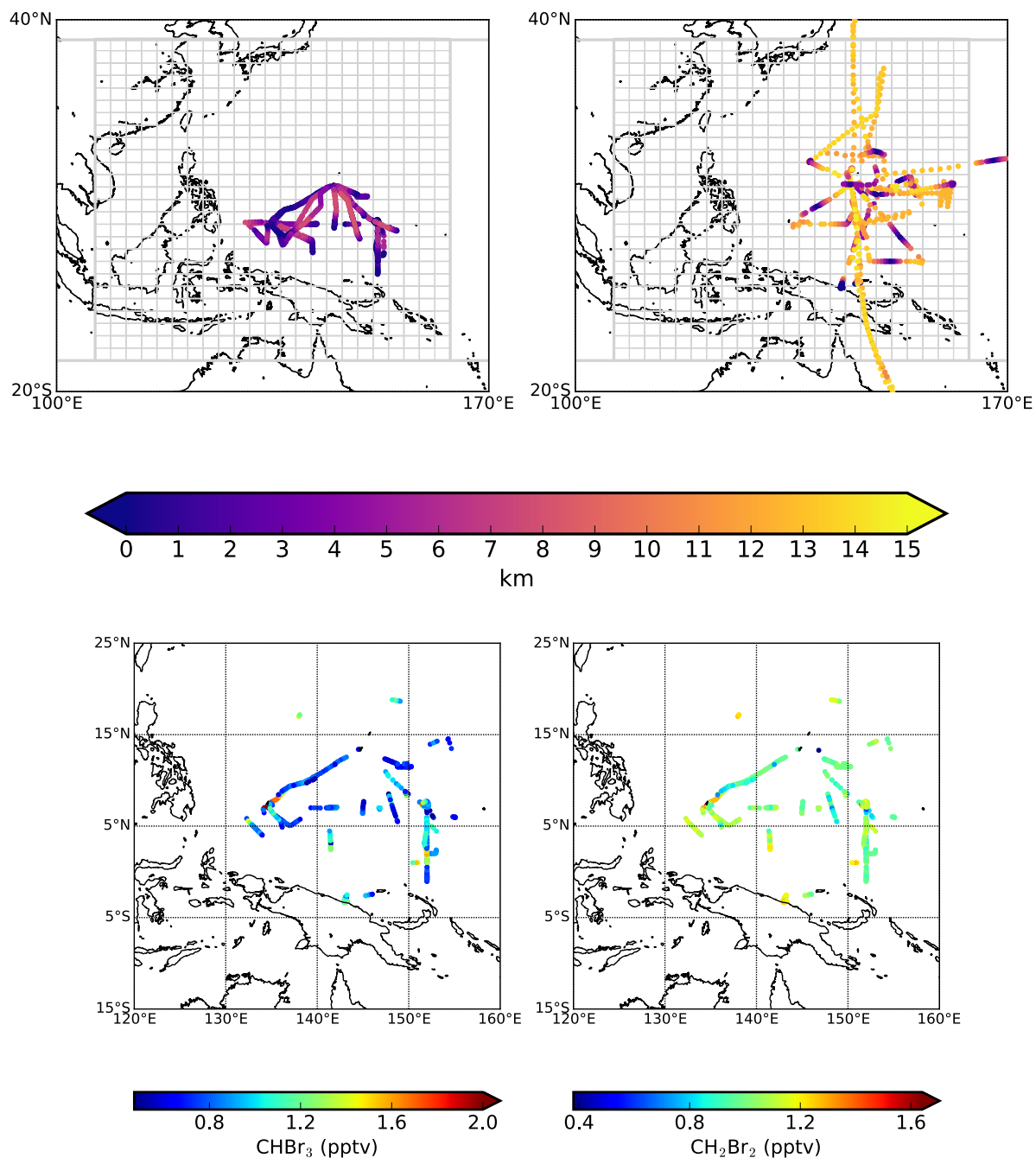
L.F, P.I.P and R.B designed the computational experiments; P.I.P. and L.F. wrote the paper; all authors provided input on data analysis shown in the paper; the CAST and CONTRAST team provided access to CHBr_3 and CH_2Br_2 data.

470 **Acknowledgements**

L.F. was funded by United Kingdom Natural Environmental Research Council (NERC) grant NE/J006203/1, R.B. was funded by NERC studentship NE/1528818/1, and P.I.P. gratefully acknowledges his Royal Society Wolfson Research Merit Award. CAST is funded by NERC and STFC, with grants NE/ I030054/1 (lead award), NE/J006262/1, 472 NE/J006238/1, NE/J006181/1, NE/J006211/1, NE/J006061/1, NE/J006157/1, NE/J006203/1, NE/J00619X/1 (University of York CAST measurements), and NE/J006173/1. We are grateful to the Harvard

University GEOS-Chem group who maintains the model. E.A. acknowledges support from NSF Grant AGS1261689 and thanks R. Lueb, R. Hendershot, X. Zhu, M. Navarro, and L. Pope for technical and engineering support. The CONTRAST experiment is sponsored by the
 480 NSF. CONTRAST data are publicly available for all researchers and can be obtained at http://data.eol.ucar.edu/master_list/?project=CONTRAST. The NOAA surface data is available at <http://www.esrl.noaa.gov/gmd/dv/ftpdata.html>.

Figures



485

Figure 1 Distributions of data from the (left) CAST and (right) CONTRAST aircraft campaigns during January and February 2014. Data are described on 2° (latitude) X 2.5° (longitude)

GEOS-Chem grid boxes. The top panels show the altitude of data collected by both campaigns. We superimpose the flux inversion domain (grey lattice), consisting of 600 grid boxes between 105°—165°E and 15S°—25°N, four larger neighbouring regions, and the rest of world. The bottom panels show the distributions of boundary layer (less than 2.5 km) CHBr₃ (pptv) and CH₂Br₂ (pptv) mole fraction data.

495

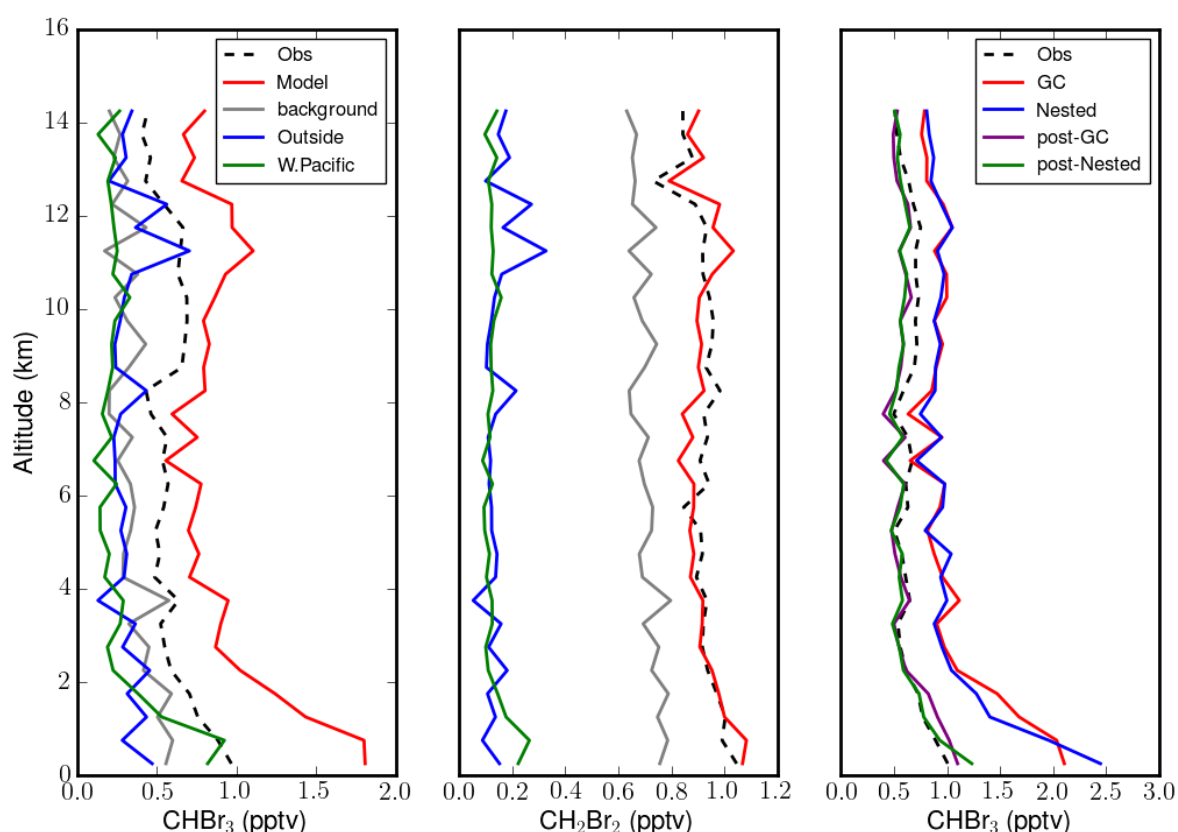


Figure 2: Observed and model mean vertical profiles of (left) CHBr₃ (pptv) and (middle) CH₂Br₂ (pptv) from the CAST and CONTRAST campaigns, described on a 1 km resolution grid. Model values have been sampled at the time and location of each observation. Also shown are the model contributions to these gases from within the Western Pacific study region, immediately outside the study region, and further afield which we denote as background values. The right panel compares CAST/CONTRAST observations of CHBr₃ with GEOS-Chem model simulations using the standard (2.0°×2.5°) and nested (0.25°×0.3125°) spatial resolutions from January 18th to February 13th, 2014. The two model runs (red and blue lines) use the same emission inventories (Ordóñez et al., 2012). For comparison, we also

500

505

present posterior model simulations (purple and green lines). based on the posterior fluxes inferred from CAST/CONTRAST observations (Figure 4).

510

515

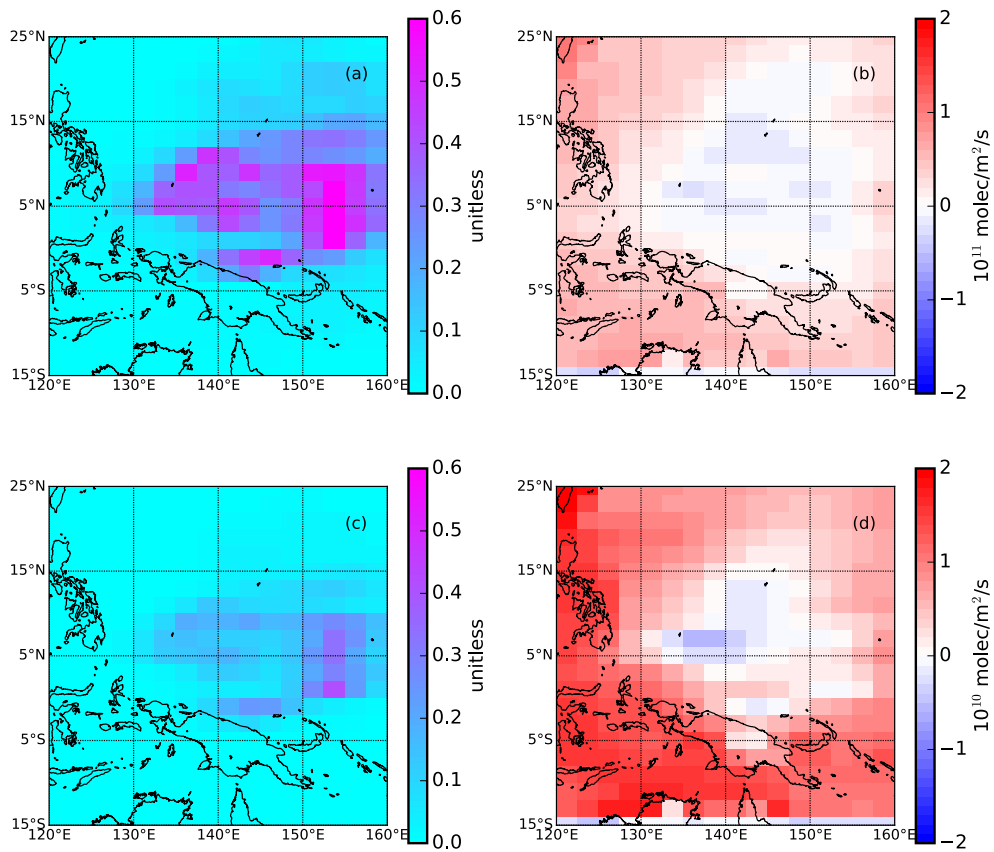
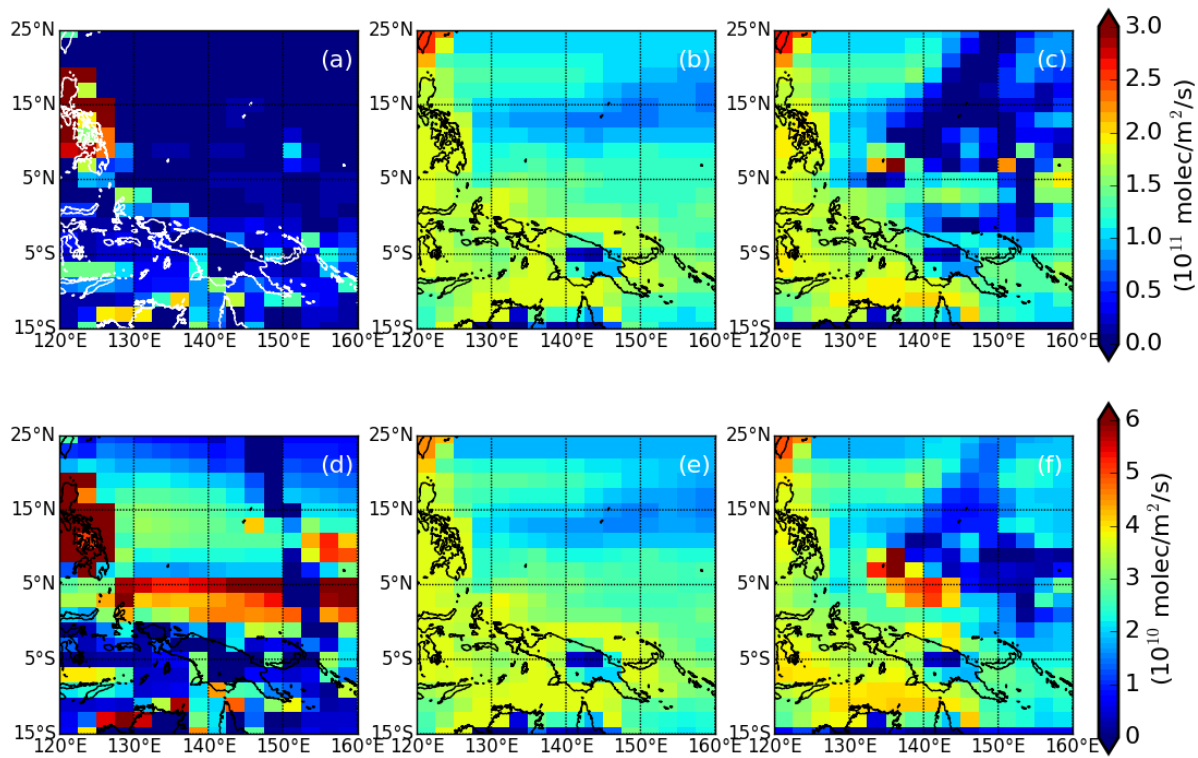


Figure 3: Simulated error reductions (unitless) and *a posteriori* flux error distributions (10^{10} molec/m²/s) of (top) CHBr_3 and (bottom) CH_2Br_2 based on the theoretical potential to recover true fluxes using the time and location of CAST and CONTRAST data.

520



525

Figure 4: *A priori* and *a posteriori* (top) CHBr₃ (10¹¹ molec/m²/s) and (bottom) CH₂Br₂ (10¹⁰ molec/m²/s) surface fluxes over the Western Pacific study region. The middle panels show the *a priori* fluxes we use in our MAP inversion (Ordóñez et al., 2012); the left panels shows an alternative bottom-up emission inventory (Ziska et al, 2013); and the right panels show our *a posteriori* flux estimates inferred from CAST and CONTRAST data.

530

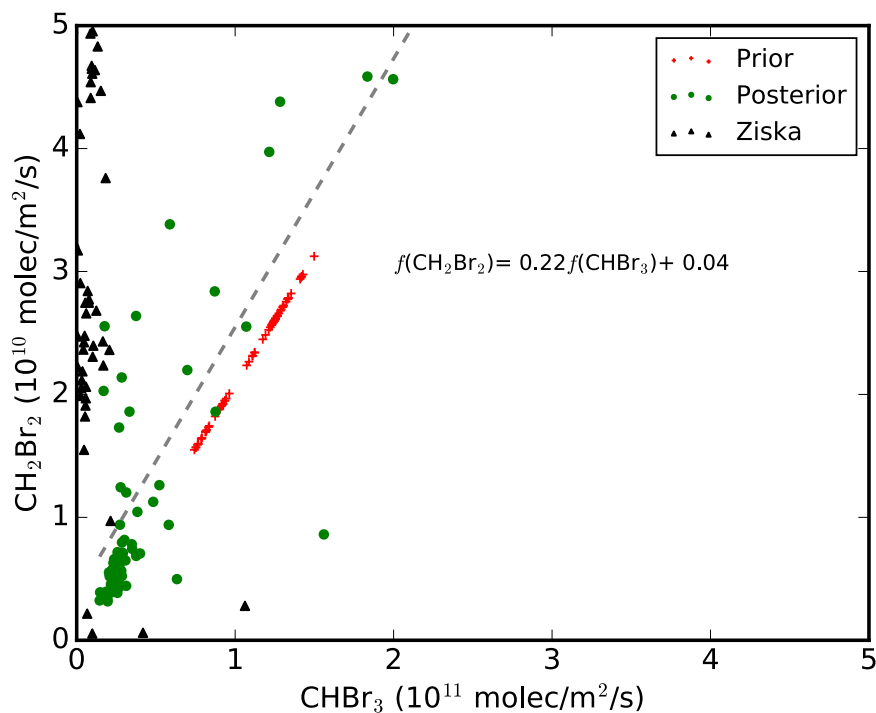
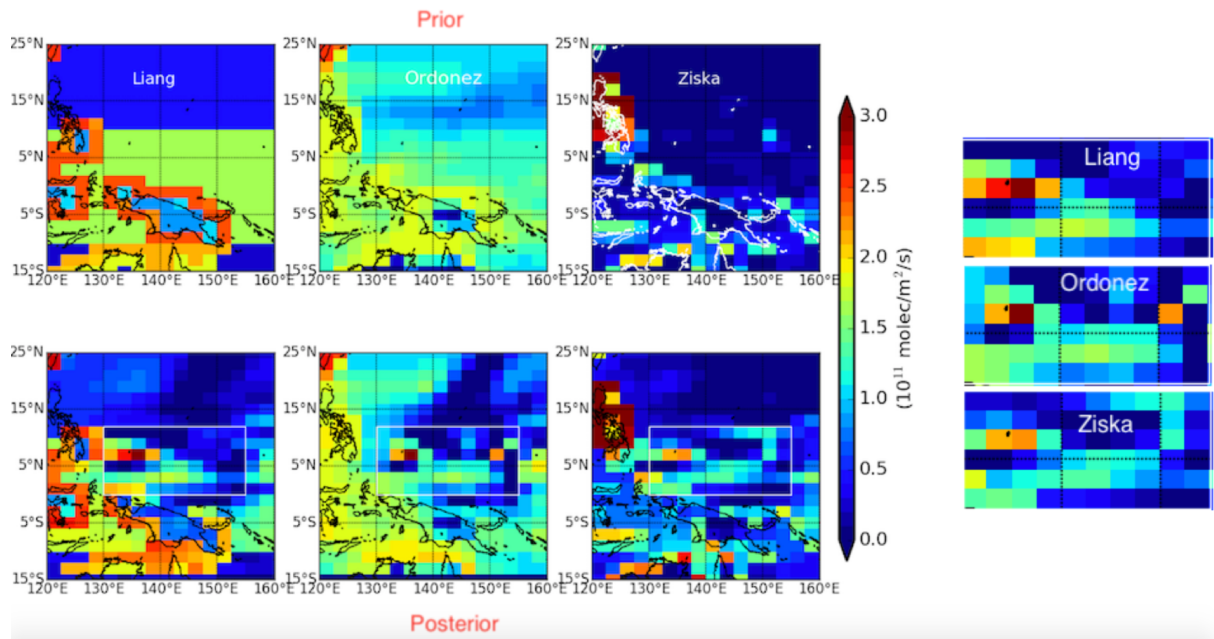


Figure 5: Scatterplot between *a priori* and *a posteriori* CHBr_3 and CH_2Br_2 fluxes described on 2° (latitude) \times 2.5° (longitude) grid boxes over a sub-region (130° — 155°E and 0° — 12°N) of the study region (Figure 1), where observations are most dense. Red crosses represent values from Ordóñez et al., 2012 that we use for our *a priori*; black triangles represent values from an alternative bottom-up inventory (Ziska et al, 2013); and green circles denote our *a posteriori* values. A *a posteriori* fluxes of CHBr_3 and CH_2Br_2 have a Pearson correlation of 0.86. The best-fit linear model for the *a posteriori* fluxes is shown inset.



550 **Figure 6:** *A priori* (left upper panels) and *a posteriori* (left lower panels) CHBr_3 flux estimates ($10^{11} \text{ molec/m}^2/\text{s}$) over the study region. The three *a priori* inventories include Liang et al (2010), Ordóñez et al (2012), and Ziska et al (2013). The right panel is focused on the geographical region $130^\circ\text{--}155^\circ\text{E}$ and $0^\circ\text{--}12^\circ\text{N}$ where CAST/CONTRAST data density was highest.

555 **References**

Andrews, S. J., Carpenter, L. J., Apel, E. C., Atlas, E., Donets, V., Hopkins, J. F., Hornbrook, R. S., Lewis, A. C., Lidster, R. T., Lueb, R., Minaeian, J., Navarro, M., Punjabi, S., Riemer, D., and Schauffler, S.: A comparison of very short-lived halocarbon (VSLs) and DMS aircraft
560 measurements in the Tropical West Pacific from CAST, ATTREX and CONTRAST, Atmospheric Measurement Techniques Discussions, 2016, 1–23, doi:10.5194/amt-2016-94, <http://www.atmos-meas-tech-discuss.net/amt-2016-94/>, 2016.

Aschmann, J., Sinnhuber, B.-M., Atlas, E. L., and Schauffler, S. M.: Modeling the transport of
565 very short-lived substances into the tropical upper troposphere and lower stratosphere, Atmos. Chem. Phys., 9, 9237–9247, doi:10.5194/acp-9-9237-2009, 2009.

Ashfold, M. J., Harris, N. R. P., Manning, A. J., Robinson, A. D., Warwick, N.J., and Pyle, J. A.: Estimates of tropical bromoform emissions using an inversion method, Atmos. Chem.
570 Phys., 14, 979–994, doi:10.5194/acp-14-979-2014, 2014.

Butler, J. H., King, D. B., Lobert, J. M., Montzka, S. A., Yvon-Lewis, S. A., Hall, B. D., Warwick, N. J., Mondeel, D. J., Aydin, M., and Elkins, J. W.: Oceanic distributions and emissions of short-lived halocarbons, Global Biogeochem. Cy., 21, GB1023, doi:10.1029/2006GB002732,
575 2007.

Butler, R., Palmer, P. I., Feng, L., Andrews, S. J., Atlas, E. L., Carpenter, L. J., Donets, V., Harris, N. R. P., Montzka, S. A., Pan, L. L., Salawitch, R. J., and Schauffler, S. M.: Quantifying the vertical transport of CHBr_3 and CH_2Br_2 over the Western Pacific, Atmos. Chem. Phys. Discuss., doi:10.5194/acp-2016-936, in review, 2016.
580

Carpenter, L. J. and Liss, P. S.: On temperate sources of bromoform and other reactive organic bromine gases, J. Geophys. Res.-Atmos., 105, 20539–20547, doi:10.1029/2000JD900242, 2000.
585

Carpenter, L. J., Jones, C. E., Dunk, R. M., Hornsby, K. E., and Woeltjen, J.: Air-sea fluxes of biogenic bromine from the tropical and North Atlantic Ocean, Atmos. Chem. Phys., 9, 1805–5
1816, doi:10.5194/acp-9-1805-2009, 2009.

590 Carpenter, L. J., Reimann, S., Burkholder, J. B., Clerbaux, C., Hall, B.D., Hossaini, R., Laube, J. C., and Yvon-Lewis, S. A.: Update on ozone-depleting substances (ODSs) and other gases of interest to the Montreal protocol, *Scientific Assessment of Ozone Depletion: 2014*, 2014.

Dorf, M., Butz, a., Camy-Peyret, C., Chipperfield, M. P., Kritten, L., and Pfeilsticker, K.:
595 Bromine in the tropical troposphere and stratosphere as derived from balloon-borne BrO observations, *Atmos. Chem. Phys. Discuss.*, 8, 12 999–13 015, doi:10.5194/acpd-8-12999-2008, <http://www.atmos-chem-phys-discuss.net/8/12999/2008/>, 2008.

Feng, L., Palmer, P. I., Bösch, H., and Dance, S.: Estimating surface CO₂ fluxes from space-
600 borne CO₂ dry air mole fraction observations using an ensemble Kalman Filter, *Atmos. Chem. Phys.*, 9, 2619-2633, <https://doi.org/10.5194/acp-9-2619-2009>, 2009.

Gschwend, P. M., Macfarlane, J. K., and Newman, K. A.: Volatile halogenated organic
605 compounds released to seawater from temperate marine macroalgae, *Science*, 227, 1033–1035, doi:10.1126/science.227.4690.1033, 1985.

Harris, N. R. P., Carpenter, L. J., Lee, J. D., Vaughan, G., Filus, M. T., Jones, R. L., Ouyang, B., Pyle, J. A., Robinson, A. D., Andrews, S. J., Lewis, A.C., Minaeian, J., Vaughan, A., Dorsey, J. R., Gallagher, M., Le Breton, M., Newton, R., Percival, C. J., Ricketts, H. M. A.,
610 Bauguitte, S. J.-B., Nott, G. J., Wellpott, A., Ashfold, M. J., Flemming,; Butler, R., Palmer, P. I., Kaye, P. H., Stopford, C., Chemel, C., Boesch, H., Humpage, N., Vick, A., MacKenzie, A. R., Hyde, R., Angelov, P., Meneguz, E., Manning, A. J., Co-ordinated Airborne Studies in the Tropics (CAST). *Bull. Amer. Meteor. Soc.*, 98, 145-162, doi:10.1175/BAMS-D-14-00290.1, 2017.

615 Hosking, J. S., Russo, M. R., Braesicke, P., and Pyle, J. A.: Modelling deep convection and its impacts on the tropical tropopause layer, *Atmos. Chem. Phys.*, 10, 11175–11188, doi:10.5194/acp-10-11175-2010, 2010.

620 Hossaini, R., Chipperfield, M. P., Feng, W., Breider, T. J., Atlas, E., Montzka, S. A., Miller, B. R., Moore, F., and Elkins, J.: The contribution of natural and anthropogenic very short-lived species to stratospheric bromine, *Atmos. Chem. Phys.*, 12, 371–380, doi:10.5194/acp-12-25 371-2012, 2012.

625 Hossaini, R., Mantle, H., Chipperfield, M. P., Montzka, S. A., Hamer, P., Ziska, F., Quack, B., Krüger, K., Tegtmeier, S., Atlas, E., Sala, S., Engel, A., Bönisch, H., Keber, T., Oram, D., Mills,

G., Ordóñez, C., Saiz-Lopez, A., Warwick, N., Liang, Q., Feng, W., Moore, F., Miller, B. R., Marécal, V., Richards, N. A., Dorf, M., and Pfeilsticker, K.: Evaluating global emission inventories of biogenic bromocarbons, *Atmos. Chem. Phys.*, 13, 11819–11838, doi:10.5194/acp-13-11819-2013, 2013.

Hossaini, R., Chipperfield, M. P., Montzka, S. A., Rap, A., Dhomse, S., and Feng, W.: Efficiency of short-lived halogens at influencing climate through depletion of stratospheric ozone, *Nat. Geosci.*, 8, 186–190, doi:10.1038/ngeo2363, 2015.

Hossaini, R., Patra, P.K., Leeson, A. A., Krysztofiak, G., Abraham, N. L., Andrews, S. J., Archibald, A. T., Aschmann, J., Atlas, E. L., Belikov, D. A., Bönisch, H., Carpenter, L. J., Dhomse, S., Dorf, M., Engel, A., Feng, W., Fuhlbrügge, S., Griffiths, P. T., Harris, N. R. P., Hommel, R., Keber, T., Krüger, K., Lennartz, S. T., Maksyutov, S., Mantle, H., Mills, G. P., Miller, B., Montzka, S. A., Moore, F., Navarro, M. A., Oram, D. E., Pfeilsticker, K., Pyle, J.A., Quack, B., Robinson, A.D., Saikawa, E., Saiz-Lopez, A., Sala, S., Sinnhuber, B.-M., Taguchi, S., Tegtmeier, S., Lidster, R. T., Wilson, C., and Ziska, F.: A multi-model intercomparison of halogenated very short-lived substances (TransComVSLs): linking oceanic emissions and tropospheric transport for a reconciled estimate of the stratospheric source gas injection of bromine, *Atmos. Chem. Phys.*, 16, 9163–9187, doi:10.5194/acp16-9163-2016, 2016a.

Hossaini, R., Chipperfield, M. P., Montzka, S. A., Leeson, A. A., Dhomse, S. S., and Pyle, J. A.: The increasing threat to stratospheric ozone from dichloromethane, *Nat. Comm.*, 8, 15962, doi: 10.1038/ncomms15962, 2016b

Jones, C. E., Andrews, S. J., Carpenter, L. J., Hogan, C., Hopkins, F. E., Laube, J. C., Robinson, A. D., Spain, T. G., Archer, S. D., Harris, N. R. P., Nightingale, P. D., O’Doherty, S. J., Oram, D. E., Pyle, J. A., Butler, J. H., and Hall, B. D.: Results from the first national UK inter-laboratory calibration for very short-lived halocarbons, *Atmos. Meas. Tech.*, 4, 865–874, doi:10.5194/amt-4-865-2011, 2011.

Law, K. S., and W. T. Sturges: Halogenated very short-lived substances, in *Scientific Assessment of Ozone Depletion: 2006*, Global Ozone Research and Monitoring Project, Rep. 50, Chap. 2, World Meteorol. Organ., Geneva, Switzerland, 2007.

- Leedham, E. C., Hughes, C., Keng, F. S. L., Phang, S.-M., Malin, G., and Sturges, W. T.: Emission of atmospherically significant halocarbons by naturally occurring and farmed tropical macroalgae, *Biogeosciences*, 10, 3615–3633, doi:10.5194/bg-10-3615-2013, 2013.
- 665
- Levine, J. G., Braesicke, P., Harris, N. R. P., Savage, N. H., and Pyle, J. A.: Pathways and timescales for troposphere-to-stratosphere transport via the tropical tropopause layer and their relevance for very short lived substances, *J. Geophys. Res.-Atmos.*, 112, D04308, doi:10.1029/2005JD006940, 2007.
- 670
- Liu, Y., Shari A. Yvon-Lewis, Daniel C. O. Thornton, James H. Butler, Thomas S. Bianchi, Lisa Campbell, Lei Hu, and Smith, R.: Spatial and temporal distributions of bromoform and dibromomethane in the Atlantic Ocean and their relationship with photosynthetic biomass, *J. Geophys. Res. Oceans*, 118, 2169-9291, DOI: 10.1002/jgrc.20299, 2013.
- 675
- Liang, Q., Stolarski, R. S., Kawa, S. R., Nielsen, J. E., Douglass, A. R., Rodriguez, J. M., Blake, D. R., Atlas, E. L., and Ott, L. E.: Finding the missing stratospheric Br_y: a global modeling study of CHBr₃ and CH₂Br₂, *Atmos. Chem. Phys.*, 10, 2269–2286, doi:10.5194/acp10-2269-2010, 2010.
- 680
- Manley, S. L., Goodwin, K., and North, W. J.: Laboratory production of bromoform, methylene bromide, and methyl iodide by macroalgae and distribution in nearshore southern California waters, *Limnol. Oceanogr.*, 37, 1652–1659, 1992.
- 685
- Montzka, S. A. and Reimann, S.: Ozone-Depleting Substances (ODSs) and Related Chemicals, vol. Scientific Assessment of Ozone Depletion: 2010, Global Ozone Research and Monitoring Project – Report No. 52, chap. 1, World Meteorological Organization (WMO), Geneva, 2011.
- 690
- O'Brien, L. M., Harris, N. R. P., Robinson, A. D., Gostlow, B., Warwick, N., Yang, X., and Pyle, J. A.: Bromocarbons in the tropical marine boundary layer at the Cape Verde Observatory – measurements and modelling, *Atmos. Chem. Phys.*, 9, 9083-9099, doi:10.5194/acp-9-9083-2009, 2009.
- 695
- Oman, L., Douglass, D., A. R., Salawitch, R., Canty, J., T., Ziemke, P. J. R., and . Manyin : The effect of representing bromine from VLS on the simulation and evolution of Antarctic ozone, *Geophys. Res. Lett.*, 43, 9869–9876, doi:[10.1002/2016GL070471](https://doi.org/10.1002/2016GL070471), 2016.

Ordóñez, C., Lamarque, J.-F., Tilmes, S., Kinnison, D. E., Atlas, E. L., Blake, D. R., Sousa
700 Santos, G., Brasseur, G., and Saiz-Lopez, A.: Bromine and iodine chemistry in a global
chemistry-climate model: description and evaluation of very short-lived oceanic sources,
Atmos. Chem. Phys., 12, 1423–1447, doi:10.5194/acp-12-1423-2012, 2012.

Palmer, C. J. and Reason, C. J.: Relationships of surface bromoform concentrations with
705 mixed layer depth and salinity in the tropical oceans, Global Biogeochem. Cy., 23, GB2014,
doi:10.1029/2008GB003338, 2009.

Palmer, P. I., J. J. Barnett, J. R. Eyre, and S. B. Healy, A nonlinear optimal estimation inverse
method for radio occultation measurements, J. Geophys. Res., 105, 17513-17526, 2000.

710 Pan, L. L., Atlas, E. L., Salawitch, R. J., Honomichl, S. B., Bresch, J. F., Randel, W. J., Apel,
E. C., Hornbrook, R. S., Weinheimer, A. J., Anderson, D. C., Andrews, S. J., Beaton, S. P.,
Campos, T. L., Carpenter, L. J., Chen, D., Dix, B., Donets, V., Hall, S. R., Hanisco, T. F.,
Homeyer, C. R., Huey, L. G., Jensen, J. B., Kaser, L., Kinnison, D. E., Koenig, T. K., Lamarque,
715 J.-F., Liu, C., Luo, J., Luo, Z. J., Montzka, D. D., Nicely, J. M., Pierce, R. B., Riemer, D. D.,
Robinson, T., Romashkin, P., Saiz-Lopez, A., Schauffler, S., Shieh, O., Vaughan, G., Ullmann,
K., Volkamer, R., Wolfe, G., Stell, M. H., and Baidar, S.: The CONvective TRansport of Active
Species in the Tropics (CONTRAST) Experiment, B. Am. Meteorol. Soc., doi:10.1175/BAMS-
D-14-00272.1, 2016.

720 Parrella, J. P., Jacob, D. J., Liang, Q., Zhang, Y., Mickley, L. J., Miller, B., Evans, M. J., Yang,
X., Pyle, J. a., Theys, N., and Van Roozendaal, M.: Tropospheric bromine chemistry:
implications for present and pre-industrial ozone and mercury, Atmos. Chem. Phys., 12, 6723–
6740, doi:10.5194/acp-12-6723-2012, <http://www.atmos-chem-phys.net/12/6723/2012/>, 2012.

725 Penkett, S. A., Engel, A., Stimpfle, R. M., Chan, K. R., Weisenstein, D. K., Ko, M. K. W., and
Salawitch, R. J.: Distribution of halon in the upper troposphere and lower stratosphere and the
1994 total bromine budget, J. Geophys. Res.-Atmos., 103, 1513–1526,
doi:10.1029/97JD02466, 1998.

730 Pisso, I., Haynes, P. H., and Law, K. S.: Emission location dependent ozone depletion
potentials for very short-lived halogenated species, Atmos. Chem. Phys., 10, 12025–12036,
doi:10.5194/acp-10-12025-2010, 2010.

- 735 Quack, B. and Suess, E.: Volatile halogenated hydrocarbons over the western Pacific between 43°S and 4° N, *J. Geophys. Res.-Atmos.*, 104, 1663–1678, doi:10.1029/98JD02730, 1999.
- Quack, B. and Wallace, D. W. R.: Air-sea flux of bromoform: controls, rates, and implications, *Global Biogeochem. Cy.*, 17, 1023, doi:10.1029/2002GB001890, 2003.
- 740 Quack, B., Atlas, E., Petrick, G., and Wallace, D. W. R.: Bromoform and dibromomethane above the Mauritanian upwelling: Atmospheric distributions and oceanic emissions, *J. Geophys. Res.- Atmos.*, 112, D09312, doi:10.1029/2006JD007614, 2007.
- 745 Read, K. A., Mahajan, A. S., Carpenter, L. J., Evans, M. J., Faria, B. V. E., Heard, D. E., Hopkins, J. R., Lee, J. D., Moller, S. J., Lewis, A. C., Mendes, L., McQuaid, J. B., Oetjen, H., Saiz, Lopez, A., Pilling, M. J., and Plane, J. M. C.: Extensive halogen-mediated ozone destruction over the tropical Atlantic Ocean, *Nature*, 453, 1232–1235, doi:10.1038/nature07035, 2008.
- 750 Russo, M. R., Ashfold, M. J., Harris, N. R. P., and Pyle, J. A.: On the emissions and transport of bromoform: sensitivity to model resolution and emission location, *Atmos. Chem. Phys.*, 15, 14031-14040, <https://doi.org/10.5194/acp-15-14031-2015>, 2015.
- 755 Stemmler, R., Hill, K., M., and Folini, D.: Low European methyl chloroform emissions inferred from long-term atmospheric measurements, *Nature*, 433, 506–508, doi:10.1038/nature03220, 2005.
- Salawitch, R. J., Canty, T., Kurosu, T., Chance, K., Liang, Q., da Silva, A., Pawson, S.,
760 Nielsen, J. E., Rodriguez, J. M., Bhartia, P. K., Liu, X., Huey, L. G., Liao, J., Stickel, R. E., Tanner, D. J., Dibb, J. E., Simpson, W. R., Donohoue, D., Weinheimer, A., Flocke, F., Knapp, D., Montzka, D., Neuman, J. A., Nowak, J. B., Ryerson, T. B., Oltmans, S., Blake, D. R., Atlas, E. L., Kinnison, D. E., Tilmes, S., Pan, L. L., Hendrick, F., Van Roozendaal, M., Kreher, K., Johnston, P. V., Gao, R. S., Johnson, B., Bui, T. P., Chen, G., Pierce, R. B.,
765 Crawford, J. H., and Jacob, D. J.: A new interpretation of total column BrO during Arctic spring, *Geophysical Research Letters*, 37, doi:10.1029/2010GL043798, <http://dx.doi.org/10.1029/2010GL043798>, I21805, 2010.
- Stemmler, I., Hense, I., and Quack, B.: Marine sources of bromoform in the global open ocean
770 – global patterns and emissions, *Biogeosciences*, 12, 1967-1981, doi:10.5194/bg-12-1967-2015, 2015.

Sturges, W.T., Cota, G.F., and Buckley, P.T.: Bromoform emission from Arcticic ealgae, *Nature*, 358, 660–662, doi:10.1038/358660a0, 1992.

775

Tokarczyk, R. and Moore, R. M.: Production of volatile organohalogens by phytoplankton cultures, *Geophys. Res. Lett.*, 21, 285–288, doi:10.1029/94GL00009, 1994.

Warwick, N. J., Pyle, J. A., Carver, G. D., Yang, X., Savage, N. H., O'Connor, F. M., and
780 Cox, R. A.: Global modeling of biogenic bromocarbons, *J. Geophys. Res.-Atmos.*, 111, D24305, doi:10.1029/2006JD007264, 2006.

Yang, X., Cox, R. A., Warwick, N. J., Pyle, J. A., Carver, G. D., O'Connor, F. M., and Savage,
N. H.: Tropospheric bromine chemistry and its impacts on ozone: a model study, *J. Geophys.*
785 *Res.-Atmos.*, 110, D23311, doi:10.1029/2005JD006244, 2005.

Ziska, F., Quack, B., Abrahamsson, K., Archer, S. D., Atlas, E., Bell, T., Butler, J. H.,
Carpenter, L. J., Jones, C. E., Harris, N. R. P., Hepach, H., Heumann, K. G., Hughes, C.,
Kuss, J., Krüger, K., Liss, P., Moore, R. M., Orlikowska, A., Raimund, S., Reeves, C. E.,
790 Reifenhäuser, W., Robinson, A. D., Schall, C., Tanhua, T., Tegtmeier, S., Turner, S., Wang,
L., Wallace, D., Williams, J., Yamamoto, H., Yvon-Lewis, S., and Yokouchi, Y.: Global sea-to-
air flux climatology for bromoform, dibromomethane and methyl iodide, *Atmos. Chem. Phys.*,
13, 8915-8934, <https://doi.org/10.5194/acp-13-8915-2013>, 2013.